High-voltage antenna-plasma interaction in whistler wave transmission: Plasma sheath effects

P. Song,[1,2] B. W. Reinisch,[1,2] V. Paznukhov,[2] G. Sales,[2] D. Cooke,[3] J.-N. Tu,[2] X. Huang,[2] K. Bibl,[2] and I. Galkin[2]

Received 20 February 2006; revised 5 October 2006; accepted 30 October 2006; published 17 March 2007.

[1] We study the plasma sheath surrounding an antenna that transmits whistler mode waves in the inner magnetosphere in order to investigate the feasibility of conducting controlled experiments on the role of wave-particle interactions in the pitch angle diffusion of relativistic radiation belt electrons. We propose a model for an electrically short antenna-sheath-plasma system with transmission frequencies below the electron characteristic frequencies and much higher than the ion characteristic frequencies. The ion current is neglected. We analytically solve a time-dependent one-dimensional situation by neglecting the effects of the wave's magnetic field. In our model, the antenna is charged to a large negative potential during a steady transmission. Positive charge occurs in the sheath and the sheath is free of electrons and conduction current. The net charge on the antenna and in the sheath is zero. The volume, or the radius in a cylindrical case, of the sheath varies in response to the charge/voltage variation on the antenna. The oscillating radius of the sheath translates to a current in the plasma, which radiates waves into the plasma. A whistler wave transmission experiment conducted by the RPI-IMAGE has shown that the model may describe the most important physical processes occurring in the system. The system response is predominately reactive, showing no evidence for significant sheath current or sheath resistance. The negligibly small sheath conduction electron current can be understood if the antenna is charged to a substantial negative potential, as described by the model. Quantitatively, the model may underestimate the sheath capacitance by about 20%.

Citation: Song, P., B. W. Reinisch, V. Paznukhov, G. Sales, D. Cooke, J.-N. Tu, X. Huang, K. Bibl, and I. Galkin (2007), High-voltage antenna-plasma interaction in whistler wave transmission: Plasma sheath effects, *J. Geophys. Res.*, *112*, A03205, doi:10.1029/2006JA011683.

1. Introduction

[2] With the increasing use of spaceborne technologies, we are becoming more and more vulnerable to space weather phenomena, among which the extremely energetic electrons in the radiation belt are a major threat [e.g., *Song et al.*, 2001]. These particles are trapped in the radiation belts with lifetimes as long as a few years, posing long-lasting threats to space-borne technologies and humans in space. Pitch angle diffusion by the wave-particle interaction is a mechanism that systematically reduces the pitch angles of the particles so that they precipitate into the atmosphere along the magnetic field lines. Theoretical investigations have shown that whistler mode waves are very efficient in pitch angle diffusion and are considered a primary candidate to reduce the relativistic electrons in the radiation belts [*Kennel and Petschek*, 1966; *Lyons et al.*, 1972; *Abel and Thorne*, 1998a, 1998b; *Albert et al.*, 2001; *Inan et al.*, 2003; *James*, 2003]. Placing a transmitter in the radiation belt to transmit whistler mode waves may be among the most direct approaches to determine the wave particle interaction.

[3] For spaceborne transmission, different from vacuum conditions, the antenna is submerged in the surrounding plasma, which is electrically highly conductive because of the low collision rate among particles in space. Here we are concerned with the case in which the plasma will allow the whistler mode to propagate. The whistler mode frequencies lie between the electron gyrofrequency and the lower-hybrid frequency when the electron plasma frequency is higher than the electron gyrofrequency [e.g., *Kivelson and Russell*, 1995]. When the antenna transmits, the two branches of a dipole antenna, if electrically insulated from the surrounding plasma, are charged alternatingly with equal but opposite voltages, forming an electric field surrounding the antenna from one branch to the other and in the surrounding space. The charged particles move in response to the electric field; the electrons are attracted to the positively charged branch of the antenna and the ions to the negatively charged

[1] Environmental, Earth, and Atmospheric Sciences Department, University of Massachusetts, Lowell, Massachusetts, USA.
[2] Center for Atmospheric Research, University of Massachusetts, Lowell, Massachusetts, USA.
[3] Air Force Research Laboratory, Space Vehicles Directorate, Hanscom Air Force Base, Massachusetts, USA.

0148-0227/07/2006JA011683

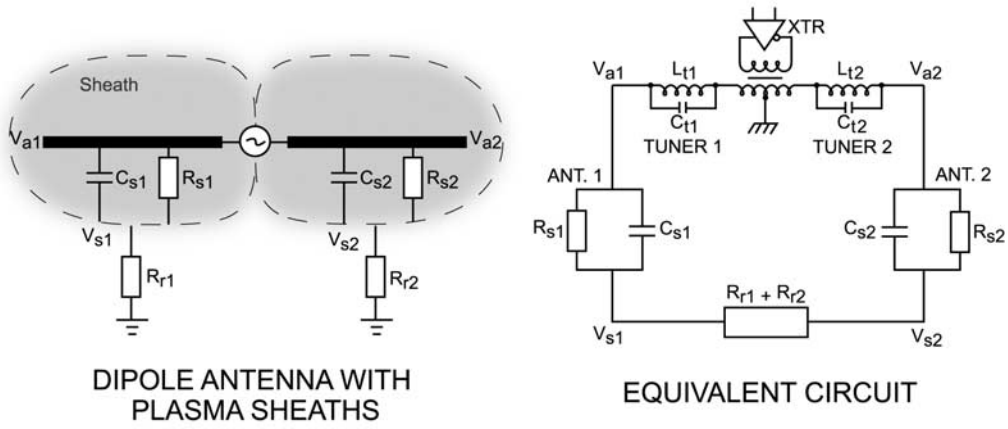

Figure 1. A transmitter-antenna-sheath-plasma system (left) and its equivalent circuit (right). In the right panel, the transmitter is expanded to include a transmitter source and a couple of tuners, the function of which is discussed in section 4. R_r is the radiation resistance, C_s and R_s are the sheath capacitance and resistance, and V_a and V_s are voltages at the antenna and at the boundary between the sheath and plasma, respectively. Note that only the circuit current, the antenna voltage V_a, and the voltage at the transmitter source (before tuner) can be measured.

branch. Furthermore, the transmission current, which flows along the antenna, generates a magnetic field. The magnetic field in turn affects the motion of the charged particles. The theories of whistler mode wave transmission in plasma can be found in numerous studies [e.g., *Arbel and Felsen*, 1963; *Balmain*, 1964; *Wang and Bell*, 1972]. Nonetheless, these theories treated regions far from the antenna.

[4] For whistler mode transmission, a substantial space-charge sheath will form around the antenna because of the different speeds with which the ions and electrons respond to the varying electric field. The quasi-neutrality approximation used in plasma theory, such as in VLF wave radiation and propagation, is no longer valid in the sheath. Figure 1 illustrates such a transmitter-antenna-sheath-plasma system and its equivalent circuit, assuming that the transmitter drives the antennas through a transformer. In the right panel, the equivalent circuit, the transmitter is expanded to a transmitter source and a couple of tuners. The tuners are not important for the discussion of the physical processes of the sheath, but they are important for transmission experiments that will be discussed in section 4. The sheath confines the electric field and functions as a shield that hinders the electromagnetic field from being transmitted. In a steady transmission, this shielding leaves only displacement currents, a small sheath leakage (conduction) current, and the magnetic component to couple to the plasma. Quantitative understanding of the sheath processes and the controlling factors is crucial to the design of a space-borne whistler wave transmitter.

[5] With a bare antenna that is not insulated from the surrounding plasma, two important processes take place: conduction currents flowing in and out of the antenna and electric charging of the antenna. Most existing theories treat a single conductor [e.g., *Laframboise and Parker*, 1973]. A transmission antenna has an active internal driver. During transmission, the positive branch collects electrons and the negative branch collects ions. Owing to the difference in ion and electron masses, electrons move faster and carry more currents than ions. The evolving DC negative antenna potential, which reduces the electron current while increasing the ion current, maintains overall charge conservation. If the two branches of the antenna are DC connected, they will share the same DC voltage. Their DC voltages can be different if they are not DC connected and are made of different materials. In our discussion below, we assume the two branches are made of the same material of high electric conductivity and are DC connected as shown in Figure 1. In a highly simplified picture, the current balance between identical positive and negative elements will be achieved at a voltage ratio of $-(m_e/m_i)^{1/2}$, for a two-branch antenna system at the peak of a wave cycle. In this case, the DC negative voltage thus can be close to the amplitude of the AC voltage. The real situation can involve other effects, such as charge collection by the spacecraft body, transition to a spherical sheath at high voltage, overlapping-sheaths, and electron emission by the negative branch due to secondary and photoelectrons, but the average or common potential is still overwhelmingly negative. The antenna-driving current now couples to the plasma through both conducted particle currents and a displacement or reactive current through the sheath capacitance. For simplicity of language we identify this reactive current with radiation into the whistler modes, while recognizing that there still remains a formidable problem to quantify the partition of the reactive current into radiating and dissipating components beyond the sheath. The electric charging of the antenna substantially changes the processes surrounding the antenna, the electrical characteristics of the antenna, and the satellite environment. Therefore to understand antenna charging is extremely important for antenna and satellite-system designs. A precise determination of the common potential requires a three-dimensional numerical analysis (e.g., Mandel, private communication, 2002, for electrostatic cases).

[6] Our present theoretical understanding of the plasma sheath processes for whistler mode transmission is built upon earlier work by *Mlodnosky and Garriott* [1962], *Despain* [1966], *Miller* [1967], *Grard and Tunaley* [1968], *Johnston* [1969], and especially that of *Shkarofsky* [1972]. *Shkarofsky* used the *Langmuir and Mott-Smith*

[1924] method to calculate the electric potential surrounding a one-dimensional static high-voltage antenna. In his model, particles are accelerated by the electric field, and particle motions produce currents. From the relationship between the current and voltage, the sheath capacitance and resistance are derived. *Oliver et al.* [1970] conducted some experiments and found substantial differences between the experiments and theory.

[7] The physical processes we will describe are fundamentally different from the previous models. Most of these models are electrostatic in which the electric field is treated as constant. In a time dependent process, such as a wave, a model not only has to describe an instant but also the very next moment in a continuous manner. To illustrate the inadequacy of a static model, let us consider the moment of maximum voltage at the antenna when all electrons in the sheath are collected by the positively charged antenna branch. In the next moment when the branch voltage is still positive but decreases and the sheath radius decreases, there are no more electrons in the sheath available for the antenna to collect any current. This is an inconsistency in a static model where the time dependence is not self-consistently included in the model because it still predicts a large current. Our model also treats the boundary conditions at the antenna surface to allow surface charging. Most importantly, our model describes a completely different physical process for the radiation current. For simplicity, in our model the ion density is approximated as frozen at the ambient density, allowing for only a small ion current to still be conducted. This particular situation allows the formation of well-defined plasma sheaths, which in our model can be treated by analytic methods and electrically approximated with a lumped circuit model as illustrated in Figure 1.

[8] In section 2 of this paper, we outline the general treatment and boundary conditions for such an antenna-plasma system. Since it is nearly impossible to solve the equation set analytically in three-dimensions, we solve the time-depend equation set in one-dimension in section 3 by neglecting the effects of the magnetic field and ions, but including antenna charge and radiation load which were not included in previous models. In section 4, we present the results from a space transmission experiment and compare them with theory.

2. General Treatment and Physical Model

2.1. Governing Equations

[9] There are three domains in the antenna-plasma system: the antenna, the sheath, and the plasma. The governing equations are different in the three domains. The solutions for each domain depend on the boundary conditions with its neighboring domains. This dependence is important because the solutions in the plasma, when calculating radiation for example, depend on the current at the sheath boundary and not the currents at the antenna surface. Between the sheath and plasma, a transition called presheath is often discussed in the literature, but for our purpose, we assume that the transition between the two domains is sharp, of the order of an electron gyroradius.

[10] Different from previous works, we take a first-principles approach, starting with Maxwell's equations and the momentum equation of electrons, neglecting the ion motion,

$$m_e d\mathbf{u}_e/dt = -e(\mathbf{E} + \mathbf{u}_e \times \mathbf{B}), \tag{1}$$

where m_e, e, $\mathbf{u}_e$, $\mathbf{E}$, and $\mathbf{B}$ are electron mass, elementary electric charge, the electron velocity, and the electric and magnetic fields, respectively. We assume that the current is carried by electrons and neglect the thermal motion of the electrons. Note that the momentum equation describes the motion of the particles in the plasma or sheath but not on the antenna. Because the spatial scale of the sheath is limited, electrons in the regions far from the sheath-plasma boundary in the sheath would hit the antenna or be pushed out of the sheath in no time. The electron momentum equation describes the motion of an electron for only a small fraction of the time of interest, during which ions are barely moved.

[11] The electric scalar potential Φ and the magnetic vector potential $\mathbf{A}$, from Maxwell's equations and the Coulomb gauge, satisfy

$$\begin{aligned} &\nabla^2\Phi = e(N - N_0)/\varepsilon_0 \\ &\nabla^2\mathbf{A} - \varepsilon_0\mu_0\frac{\partial^2\mathbf{A}}{\partial t^2} - \varepsilon_0\mu_0\frac{\partial\nabla\Phi}{\partial t} = -\mu_0\mathbf{J}, \end{aligned} \tag{2}$$

where N_0, N, $\mathbf{J}$, ε_0, and μ_0, are the number density of the ion or background plasma number density, electron density, electric current, dielectric constant, and magnetic permeability in vacuum. We have assumed that ions are singly charged. The electric charge conservation equation can be obtained from the combination of Ampere's law and Poisson's equation and is

$$\partial\rho_q/\partial t + \nabla \bullet \mathbf{J} = 0, \tag{3}$$

where $\rho_q = e(N_0 - N)$ is the net electric charge density.

2.2. Boundary Conditions at the Antenna Surface

[12] The boundary conditions at the antenna surface are crucial to describe the antenna charging and have not been treated in previous models [e.g., *Shkarofsky*, 1972]. Inside the antenna, both the electric and magnetic fields are zero if one assumes that the antenna is perfectly conducting. The current flows and electric charges occur on the surface of the antenna. At the antenna surface, the boundary conditions are

$$\begin{aligned} &E_{na^+} - E_{na^-} = E_{na^+} = \sigma_a/\varepsilon_0 \\ &\mathbf{E}_{Ta^+} = \mathbf{E}_{Ta^-} = 0 \\ &B_{na^+} = B_{na^-} = 0 \\ &\mathbf{B}_{Ta^+} - \mathbf{B}_{Ta^-} = \mathbf{B}_{Ta^+} = \mu_0\boldsymbol{\alpha}_a \times \mathbf{n}, \end{aligned} \tag{4}$$

where subscripts T and n denote the components tangential and normal to the antenna surface, the plus and minus signs denote values on the sheath and antenna sides of the boundary, respectively, σ_a is the surface charge density on the antenna, and vectors $\mathbf{n}$ and $\boldsymbol{\alpha}_a$ are the normal direction of the antenna surface and the surface current density on the antenna, respectively.

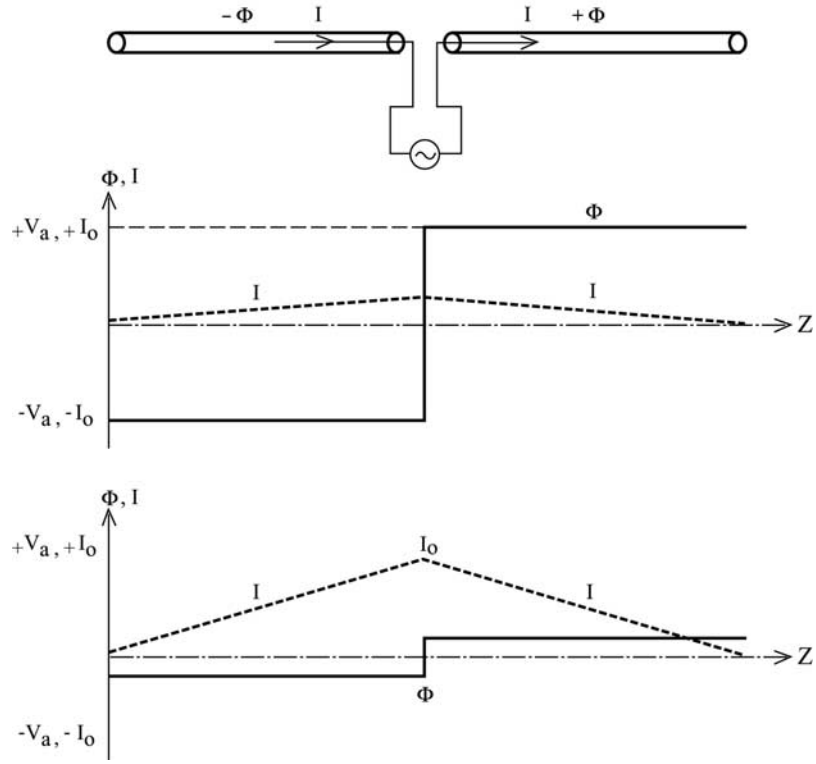

Figure 2. Temporal and spatial variations of the voltage and current on the antenna. Top panel shows the transmitter and antenna system. The transmitter, which includes the driving source and the tuners, drives a current into the antenna. The two lower panels show the current (thick dashed lines) and voltage (thick solid lines) at different times as functions of z along the antenna.

[13] For an antenna that is much shorter than the wavelength and is driven by a sinusoidal voltage oscillation of amplitude V_0, the antenna voltage is

$$V_a(z,t) = \mathrm{sgn}(z) V_0\, e^{j\omega t} + V_{a0}, \tag{5}$$

where V_{a0} is the DC floating voltage of the antenna, noting that each branch of the antenna is at equipotential. In the following discussion, for convenience, we discuss the positive branch of the antenna and drop the sign function in (5). For a short antenna, the antenna current, flowing on the surface of the antenna, can be approximated as linearly decreasing toward the tips of the antenna, when the end effects are neglected, or

$$I_a(z,t) = I_0(1 - |z|/l)e^{j(\omega t - \delta)}, \quad -l < z < l, \tag{6}$$

where l is the antenna half-length. There is a phase shift δ between the current and the voltage when the circuit is not purely resistive. Figure 2 illustrates the temporal and spatial relations. The top panel shows a dipole antenna at the potentials $\pm\varphi$ and the resulting current, which is approximately 90° out of phase with the potential when the antenna is predominately reactive. The middle panel shows the voltage and current as functions of distance from the center along the antenna at $t = 0$, assuming zero DC electric current. The lower panel shows the situation at a later time when the current peaks.

[14] At the antenna, for either an insulated surface or a bare-metal conducting surface in steady state transmission, the radial component of the electric current is negligible, as discussed later for a thin antenna. Assuming azimuthal symmetry, integrating the charge conservation equation (3) over the cross section of the antenna yields

$$I_0 e^{j(\omega t - \delta)} = 2\pi r_a l \frac{\partial \sigma_a}{\partial t} = j\omega 2\pi r_a l \sigma_{ai}, \tag{7}$$

where r_a is the radius of the antenna and $\sigma_a = \sigma_0 + \sigma_{ai}$. Here σ_0 and σ_{ai} are the DC and AC components, respectively. The DC component is associated with the antenna charging and the AC component due to the driving current. The AC charge is uniformly distributed on the surface and varies ~90° out of phase with the driving current and an amplitude of $I_0/2\pi r_a \omega l$. The cylindrical components of the electric field immediately outside of the antenna are

$$\begin{aligned} E_{ra^+} &= \frac{\sigma_0}{\varepsilon_0} + \frac{I_0 e^{j(\omega t - \delta)}}{j\omega\varepsilon_0 2\pi r_a l} \\ E_{\varphi a^+} &= 0 \\ E_{za^+} &= 0. \end{aligned} \tag{8}$$

The electric field is uniform along z when the end effects are neglected. Integrating the z-component of Ampere's law over the cross section of the antenna yields, noting from (8) that E_{za+} is zero,

$$\begin{aligned} B_{ra^+} &= 0 \\ B_{\varphi a^+} &= \frac{\mu_0}{2\pi r_a} I_a \;\; = \frac{\mu_0}{2\pi r_a} I_0(1 - |z|/l)e^{j(\omega t - \delta)}, \quad -l < z < l \\ B_{za^+} &= 0. \end{aligned} \tag{9}$$

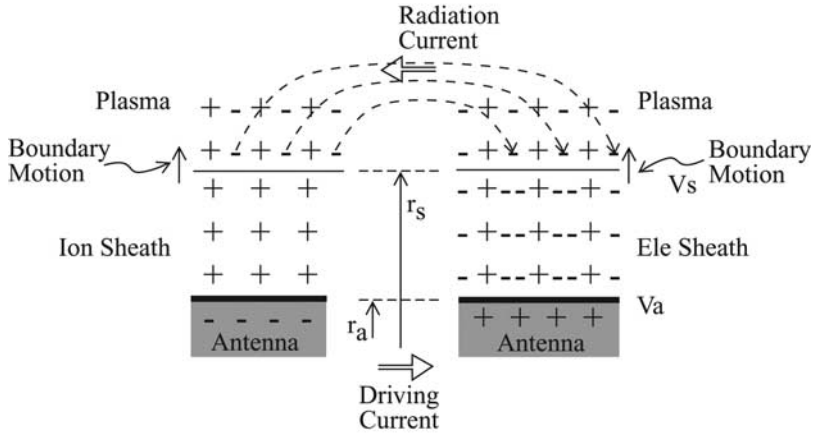

Figure 3. Physical processes in the plasma sheath surrounding an (insulated) antenna. The antenna is in a process with increasingly positive (negative) voltage on the positive (negative) branch. Dashed lines with arrowheads indicate the electron motion at a moment when the boundary between the plasma and the sheath moves up. The direction of the electric current is indicated by open arrowheads. For illustration purposes, we have made the two sheaths symmetric. In fact, the electron sheath is thinner than the ion sheath.

2.3. Electric Charging of a Bare Antenna

[15] Before we discuss the processes around a bare antenna, it is instructive to first examine the processes occurring around a perfectly insulated antenna that has no DC connection to the spacecraft body. For such antenna, because there is no conduction current flowing into the antenna from the sheath, the electrons that are pushed out from the ion-sheath side form the electron sheath on the other side (Figure 3). The temporal variation of the antenna surface charge translates into the variation of the thickness of the sheath. The electron motion in the plasma, not in the sheath, associated with the motion of the boundary produces a current in the plasma. This current corresponds to the radiation current of the antenna in a free-space setting. Since, from equation (7), the surface charge has a 90° phase shift from the driving current, the phase shift between the antenna voltage and the driving current, δ, is nearly 90° when the radiation resistance is small compared to the sheath reactance. In this case, the sheath functions in the same way as a capacitor: the two branches of the antenna are the two plates of a capacitor. The difference from a common capacitor is that the distance between the plates varies in time. The current coupled through the sheath can be interpreted as a displacement current.

[16] For a bare antenna, on the other hand, the processes near the antenna surface are different. In the first few wave cycles, there are two processes taking place: current exchange between the sheath and antenna, and electric charging of the antenna associated with the electrons that flow into or stay on the surface of the antenna.

[17] On the positively charged side, electrons are accelerated by the electric field and hit the antenna surface in no time and are stopped. The kinetic energy of the electrons is converted into thermal energy and heats the antenna. The electron sheath does not occur, given that the acceleration time for the electrons hitting the antenna is much shorter than a wave cycle. As the electrons flow into the antenna, the charge on the positively charged side is reduced. In the next half wave cycle when the voltage of the branch is negative, if photoelectron emissions are absence, the electrons will not leave the antenna and reemit into space [e.g., *Garrett*, 1985], if we neglect the possibility of ion collection from the sheath. The whole antenna becomes negatively charged with a DC voltage V_{a0}. The negative charging of the antenna enlarges the size of the ion sheath.

[18] The charging process is expected to complete in a few wave cycles. The system then reaches an equilibrium at which the minimum thickness of the ion sheath during a wave cycle is close to zero. At the moment of the minimum thickness, we note that the antenna is charged with a negative DC voltage close to the amplitude of the AC voltage and that the AC antenna voltage is nearly 90° out of phase with the current; therefore the antenna has nearly zero output in power because the driving current is near zero when the AC voltage reaches its maximum. In the equilibrium state of the transmission, the conduction current in the sheath is near zero because the sheath is nearly free of electrons as discussed before. In reality, when ion motion is included, small leakage currents may exist and satisfy,

$$\int I_i dt + \int I_e dt = 0, \tag{10}$$

where I_i and I_e are ion and electron conduction currents, respectively. It will be discussed later that the DC current is negligible.

3. One-Dimensional Cylindrical Solutions

3.1. Weak Magnetic Field Approximation

[19] In a thin cylindrical antenna (neglecting end effects), the magnetic field produced by the driving current is in the azimuthal direction varying in phase with the current and its strength decreases toward the tips of the antenna as the current becomes weaker, e.g., see equation (9). In other words, when the magnetic field is included, the magnetic field coupling makes the system no longer one-dimensional (1-D). One may easily verify from the radial component of Ampere's law that this magnetic field spatial change is due to

the displacement current associated with the antenna surface charge, while the magnetic field itself is associated with the driving current. Therefore a weak magnetic field approximation is necessary for a 1-D model. In the following we examine the order of magnitude of the magnetic field effect in the momentum equation and in Maxwell's equations.

[20] For an antenna voltage of 10^3 V and the spatial scale of the sheath of $r \sim 10^0$ m, the electric field is of the order of 10^3 V/10^0 m $\sim 10^3$ V/m. Note that this is the electric field in the sheath and is not that in the plasma wave radiated into the plasma, which is much smaller. The electron velocity is of the order of the speed accelerated by the antenna voltage, or $u_e \sim 10^7$ m/s. The amplitude of the magnetic field in the sheath associated with the antenna current is of the order of $\mu_0 I_0/2\pi r \sim 10^{-7}$ T, assuming $I_0 \sim 10^0$A. The magnetic field is therefore dominated by Earth's magnetic field, which is about 10^{-5} T depending on the altitude of the transmitter. The Coulomb force is about an order of magnitude larger than the $\mathbf{u}_e \times \mathbf{B}$ force. The effect of the wave's magnetic field in the momentum equation (1) can therefore be neglected in a zeroth-order treatment.

[21] The timescale of the acceleration of electrons is the electron plasma oscillation period when the electric field is the dominant term. An ion sheath becomes electron-free in a timescale of $r/u_e \sim 10^0/10^7 \sim 10^{-7}$ s. This is the timescale of the formation of the sheath, during which electrons are either pushed out of the sheath on one side or hit the antenna on the other side. In comparison, the period of the wave is 10^{-4} s. Essentially, there are no electrons in the ion sheath.

[22] For a transmission frequency of 10^4 Hz, the component of the electric field associated with the vector potential in (2) is of an order of 10^{-3} V/m, given the magnetic field generated by the antenna current $\mu_0 I_0/2\pi r \sim 10^{-7}$ T. If the component associated with the scalar potential is of the order of 10^3 V/m, the magnetic field term in Faraday's law can be neglected.

[23] For Ampere's law, the magnetic field spatial variations in the radial direction and along the antenna are of the order of $\sim 10^{-8\sim 9}$ T/m. The current and displacement term are of the order of 10^{-8} T/m and 10^{-9} T/m, respectively. Therefore the magnetic field term cannot be simply neglected. However, from the divergence of Ampere's law, the magnetic field term vanishes and we obtain the charge conservation equation (3). In other words, different from an electrostatic model, we include Ampere's law in our treatment. The electric field is solved with the two equations in which the time independence is implicit. The time-dependent effects are incorporated from the antenna driving boundary conditions, the charge conservation, and, to some degree, the momentum equation when it is applied to the sheath-plasma boundary, which oscillates with the driving current/voltage.

3.2. Time-Dependent Solution for Charged Bare Antenna

[24] For a thin antenna, which will be discussed, of 0.2 mm in radius and 125 $\sim$ 250 m long, the one-dimensional approximation is valid. The sheath potential equation becomes

$$\frac{1}{r}\frac{\partial}{\partial r} r \frac{\partial \Phi}{\partial r} = -\frac{eN_0}{\varepsilon_0}, \quad (r_a < r < r_s), \tag{11}$$

where r_s is the sheath radius. Note that the sheath is free of electrons, as we discussed in section 2 and the previous subsection. Also note that the equation applies only to the sheath region. A major issue for solving the problem is that the location of the sheath-plasma boundary is unknown and is a function of time. Outside of the sheath, the governing equation is different. How to determine the sheath-plasma boundary location will be discussed in section 3.3. The general solutions of the electric potential in the sheath are

$$\Phi = -\frac{eN_0}{\varepsilon_0}\left(\frac{r^2}{4} + C_1 \ln r\right) + C_2. \tag{12}$$

With the boundary conditions, (8),

$$\frac{\partial \Phi(r_{a+})}{\partial r} = -\frac{\sigma_0}{\varepsilon_0} - \frac{I_0 e^{j(\omega t-\delta)}}{j\omega 2\pi r_a l \varepsilon_0}$$
$$\Phi(r_{a+}) = V_a \tag{13}$$

the electric potential is

$$\Phi(r) = V_a - \frac{eN_0}{4\varepsilon_0}\left[r^2 - r_a^2 + \left(\frac{4\sigma_0 r_a}{eN_0} - j2a^2 e^{j(\omega t-\delta)} - 2r_a^2\right) \cdot \ln\left(\frac{r}{r_a}\right)\right], \tag{14}$$

where $r_a < r < r_s$ and

$$a^2 = \frac{I_0}{\pi\omega l e N_0}. \tag{15}$$

For the DC component

$$\Phi_0(r) = V_{a0} - \frac{eN_0}{4\varepsilon_0}\left[r^2 - r_a^2 + \left(\frac{4\sigma_0 r_a}{eN_0} - 2r_a^2\right)\ln\left(\frac{r}{r_a}\right)\right]. \tag{16}$$

The radius of the static sheath r_{s0}, at which the static voltage and static electric field go to zero, and the corresponding the surface charge and DC voltage of the antenna satisfy

$$V_{a0} = \frac{eN_0}{4\varepsilon_0}\left[r_{s0}^2 - r_a^2 - 2r_{s0}^2 \ln\left(\frac{r_{s0}}{r_a}\right)\right]$$
$$r_{s0}^2 = r_a^2 - \frac{2\sigma_0 r_a}{eN_0}. \tag{17}$$

The first expression is the same as the static result derived by *Shkarofsky* [1972]. The relationship between the DC voltage and static sheath radius as functions of plasma frequency in given in Figure 4. When the voltage is higher, the static sheath is thicker. The sheath is thinner when the plasma density is higher. From the second expression, it is obvious that the surface charge σ_0 is negative. The second expression states the fact that the total positive charge within the sheath equals the total negative charge on the antenna surface. If the antenna is very thin and the current is strong, the potential in the regions far away from the antenna is

$$\Phi(r,z,t) \approx \mathrm{sgn}(z) V_0 e^{j\omega t} + V_{a0} - \frac{eN_0}{4\varepsilon_0}\left[r^2 + \left(\frac{4\sigma_0 r_a}{eN_0} - j2a^2 e^{j(\omega t-\delta)}\right)\ln\left(\frac{r}{r_a}\right)\right], \tag{18}$$

where $r_a \ll r < r_s$.

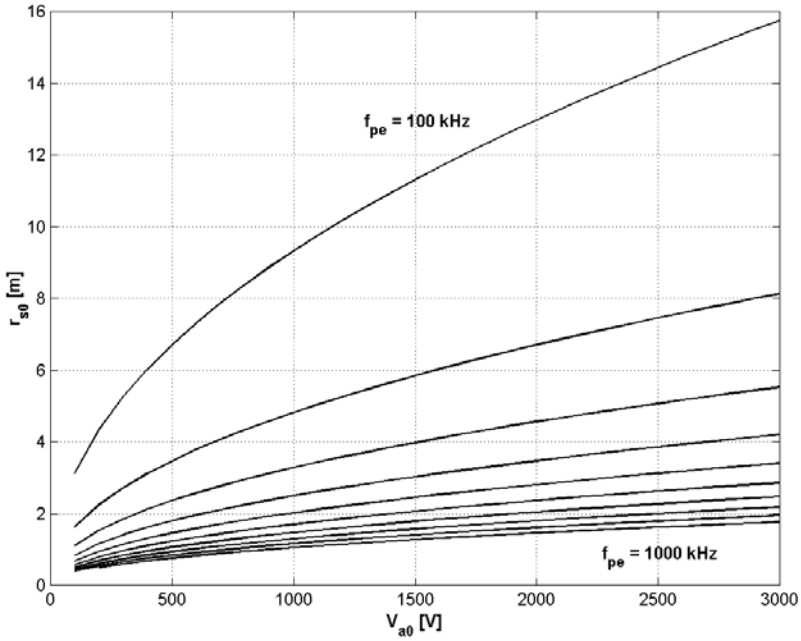

Figure 4. The relationship between the DC voltage and the static sheath radius as functions of plasma frequency. The antenna radius is assumed as 0.2 mm.

3.3. Sheath-Plasma Boundary Conditions

[25] Equation (14) gives the potential and thus the electric field throughout the sheath. It is also valid at the sheath-plasma boundary where the governing equation changes because of the presence of electrons in the plasma. However, since the location of the sheath is not defined yet, it does not specify the values at the boundary. In earlier models [e.g., *Shkarofsky*, 1972], the potential as well as electric field are taken to be zero at the sheath boundary. When there is radiation, both cannot be zero at the same time. Let us derive the boundary conditions at the sheath-plasma boundary.

[26] From the discussion above and Figure 3, the boundary is in constant motion, which translates to an electric current. Take a small column normal to and near the sheath-plasma boundary and let the boundary move from the bottomside of the column, r_s, to the topside, $r_s + dr_s$, in dt. The change in the total charge within the column during dt is $eN_0S\,dr_s$, where S is the cross section of the column. Since the height of the column dr_s is infinitely small, the current flows only normally to the sheath boundary. From the charge conservation (3), the current density flowing out of the column is

$$J_s = -eN_0 \frac{dr_s}{dt}. \tag{19}$$

The negative sign is due to the negative electron charge.

[27] Similarly, if taking a volume that coincides with the maximum size of the sheath of one branch of the antenna, the current flows into the volume along the antenna and out along the surface of r_{sm}, which is the maximum radius of the sheath. The current flowing into the surface equals that flowing out of it, according to Figure 1. It follows that while the sheath boundary oscillates within the volume, the net total charge within the volume is determined according to (3). At the moment when the current is zero, the total net charge is zero; namely, the negative charge on the antenna surface equals the total ion charge in the sheath. This zero net-charge condition holds throughout a wave cycle and it is

$$2\pi r_a l\left(-\sigma_0 - \frac{I_0 e^{j(\omega t-\delta)}}{j\omega 2\pi r_a l}\right) = eN_0 l\pi\left(r_s^2 - r_a^2\right). \tag{20}$$

Combining (20) with (17) yields

$$r_s^2 = r_{s0}^2 + ja^2 e^{j(\omega t-\delta)}. \tag{21}$$

The sheath thickness is 90° out of phase with the current and, however, is not exactly in phase with the voltage when there is radiation resistance. The total current flowing from the sheath into the plasma equals the radiation current, and is, by combining (21), (19), and (15),

$$I_{rad} = I_s = \int_0^l 2\pi r_s J_s dz = I_0 e^{j(\omega t-\delta)}. \tag{22}$$

In other words, the radiation current equivalence to that defined in radiation theory without the plasma sheath is now the current associated with the sheath boundary motion and equals the total driving current. In 1–D and neglecting the end effects, the sheath current is uniformly distributed along the extent of the antenna instead of having a decreasing magnitude toward the tips as on the antenna surface, as specified in (6). Furthermore, it is normal instead of tangential to the surface for a thin antenna.

[28] The electric field at the boundary appears to be zero when combining (21) with the derivative of (14) with

respect to r. The electric potential at the sheath boundary is, however, not zero and is

$$V_s = \Phi(r_s) = V_a - \frac{eN_0}{4\varepsilon_0}\left[r_s^2 - r_a^2 + \left(\frac{2\sigma_0 r_a}{eN_0} - ja^2 e^{j(\omega t-\delta)} - r_a^2\right)\cdot \ln\left(\frac{r_s^2}{r_a^2}\right)\right] = V_0 e^{j\omega t} + \frac{eN_0}{4\varepsilon_0}\left[-ja^2 e^{j(\omega t-\delta)} - r_{s0}^2 \ln\left(\frac{r_{s0}^2}{r_a^2}\right) + \left(r_{s0}^2 + ja^2 e^{j(\omega t-\delta)}\right)\ln\left(\frac{r_{s0}^2 + ja^2 e^{j(\omega t-\delta)}}{r_a^2}\right)\right]. \quad (23)$$

3.4. Sheath Reactance and Radiation Resistance

[29] In our circuit, Figure 1, neglecting the sheath loss, the AC voltages and current at a frequency ω satisfy

$$\begin{aligned} V_a - V_{a0} &= V_0 e^{j\omega t} = (R_r + jX_s) I_0 e^{j(\omega t-\delta)} \\ V_s &= V_{s0} e^{j(\omega t-\delta)} = R_r I_0 e^{j(\omega t-\delta)} \\ R_r + jX_s &= \sqrt{R_r^2 + X_s^2}\, e^{j\delta}, \end{aligned} \quad (24)$$

where $X_s = -1/\omega C$ and R_r are the reactance of the sheath and the radiation resistance of a branch, respectively. Separating the real and imaginary parts in (23) and combining with (24) yields

$$\begin{aligned} V_{s0} &= \frac{R_r}{\sqrt{R_r^2 + X_s^2}} V_0 = R_r I_0 \\ X_s &= -\frac{1}{2\pi\omega l \varepsilon_0}\left[\ln\left(\frac{r_s}{r_a}\right) - \frac{1}{2}\right]. \end{aligned} \quad (25)$$

We have assumed that the temporal variation in the logarithm of the sheath radius affects only the amplitude and not the phase. When the sheath is much thicker than the antenna, the capacitance of the sheath is similar to that of a coaxial cable with a radius r_s. Since the radius of the cable in this case varies during a wave cycle, the capacitance of each branch varies with time. When the two branches are treated as a single system, the two capacitances vary out of phase and the total capacitance varies less dramatically.

[30] The radiation resistance of a branch of the antenna is

$$R_r^2 = \left(\frac{V_0}{I_0}\right)^2 - X_s^2. \quad (26)$$

The two branches of the antenna may not be the same in length. However, their DC voltages are the same as discussed earlier in the introduction, assuming that they are made of the same highly conducting materials. Since the amplitude of the sheath radius is a function of length, the sheaths may oscillate at different ranges for the two branches. For a fully charged antenna, the minimum of the sheath radius is limited by the antenna radius, or

$$r_{sm}^2 = r_{s0}^2 - a_m^2 \geq r_a^2, \quad (27)$$

where a_m is the amplitude of the shorter branch l_m. For the shorter (longer) branch, the equal (greater than) sign applies. As the two sheath reactances are in series and vary both in time with a 180° phase difference, the average reactance is

$$\overline{X}_s = \frac{1}{T_w}\int_0^{T_w} (X_{s1} + X_{s2})\, dt, \quad (28)$$

where $T_w = 1/f$ is the period of the wave. Combining with (28), (25), and (21), the total sheath reactance is

$$\overline{X}_s = -\frac{1}{\omega \overline{C}} = -\frac{1}{4\pi\omega\varepsilon_0}\left(\frac{1}{l_1} + \frac{1}{l_2}\right)\left[\ln\left(\frac{I_0}{\pi\omega l_m e N_0 r_a^2} + 2\right) - 1\right]. \quad (29)$$

4. Sheath Capacitance Measurements: Space-Borne VLF Transmission Experiment

[31] In order to verify the theoretical model, we conducted an experiment using the Radio Plasma Imager (RPI) [*Reinisch et al.*, 2000] on the IMAGE satellite [*Burch et al.*, 2001] operating in the inner magnetosphere. The RPI antenna is cylindrical and was made of copper. Its radius r_a is 0.2 mm and the two branches are 250 m and 125 m long, respectively. The RPI antennas share a common DC ground with the satellite. As the antenna is charged, the satellite will be charged to the same voltage. The RPI tuners consist of a combination of inductors and capacitors selected in a way that minimizes the relay switching requirements when the transmitter frequency varies over the frequency range from 3 to 200 kHz. The net reactance of the tuner is positive (inductive) to "tune out" the negative (capacitive) reactance of the antenna. The objective of the experiment was to measure the sheath impedance during whistler wave transmission by varying the tuner inductance and transmission frequency and looking for "tuned transmission," during which the antenna current maximizes and, as a consequence, generates a voltage maximum at the antenna. Figure 5 shows the RMS antenna AC currents and voltages at the two antenna branches, +X and −X, for frequencies between 8 and 22 kHz during a 3-hour transmission period. The RPI design does not allow changing the tuner inductance without changing the frequency, so we were forced in our experiment to change the frequency. Each frequency was transmitted with a fixed inductance, and inductances at different frequencies may be different. Therefore unfortunately, the frequency and inductance effects are intertwined. In the experiment, RPI stepped through a set of inductances in 1.25 min, and repeated the procedure every 4 min. For each inductance (and frequency), more than 800 wave cycles were transmitted. If the antenna charging took a few wave cycles, the transient processes during charging contributed little to the measurements, which were therefore assumed to be made when the antenna was charged. Between two scans, regular sounding and dynamic spectra were made in order to determine the plasma conditions at the spacecraft location. The plasma frequency and electron gyrofrequency measured by local resonances [*Reinisch et al.*, 2001; *Benson et al.*, 2003] are given in Figure 6.

[32] Clear enhancements in the current and voltage amplitudes are seen at some frequencies (inductances) in Figure 5. As discussed before, the enhancements at these frequencies

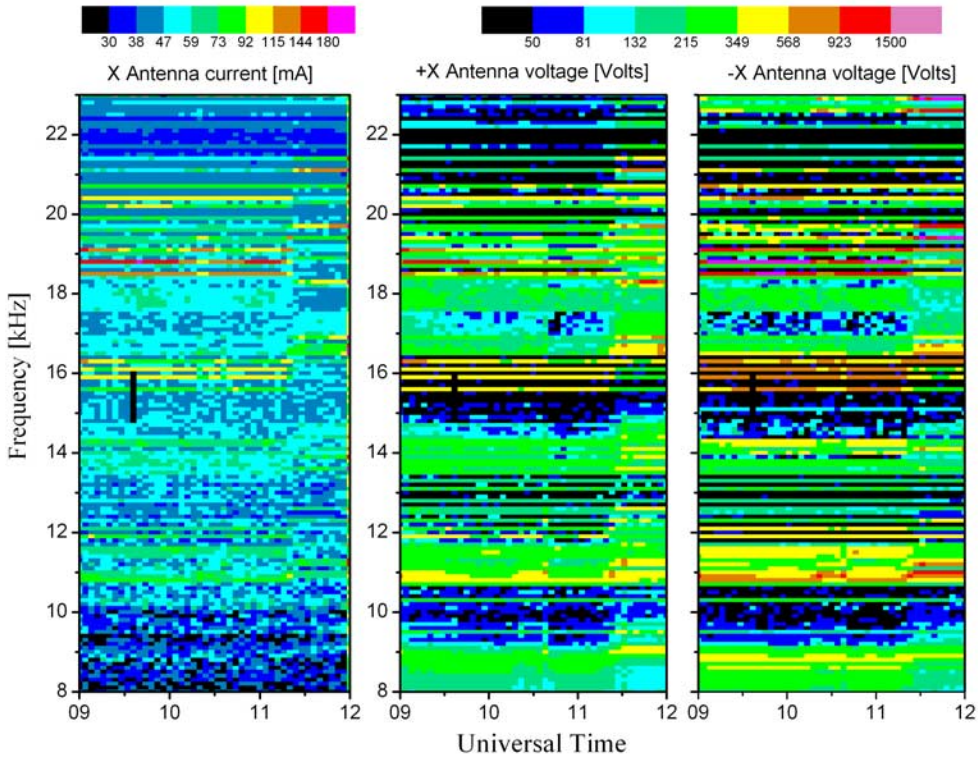

Figure 5. Current and voltages as functions of frequency (inductance) and time on the X-antenna, measured by RPI on 29 September 2004 during a whistler wave transmission experiment. The color-coding shows the RMS amplitude.

were the result of specific inductance/frequency combinations. In addition, the plasma conditions varied as the satellite moved from one region to another as shown in Figure 6. Between 0930 and 1130 UT the transmission frequencies satisfy the whistler mode condition. The analysis provided below separates the effects of the frequency and plasma density.

[33] RPI does not measure the phase between the current and voltage. The absolute values of the amplitudes are not precisely calibrated, but the relative variations are real. Nevertheless, since the sheath reactance depends only on the logarithm of the current, the uncertainty in the absolute value of the current will not significantly affect the results of the analysis. When the antenna is correctly tuned, the maximum current into the antenna was measured as 0.2 A when the antenna voltage was close to 3 kV. If the sheath admittance were dominated by the sheath conductance ($1/R_s$ in Figure 1) and the susceptance were relatively small, i.e., if $\omega C_s \ll 1/R_s$, the antenna voltage and current would approximately be in phase and the power dissipation in the antenna close to 600 VA, split between R_s, the tuner resistance R_t, the radiation resistor with $R_t + R_r \ll R_s$.

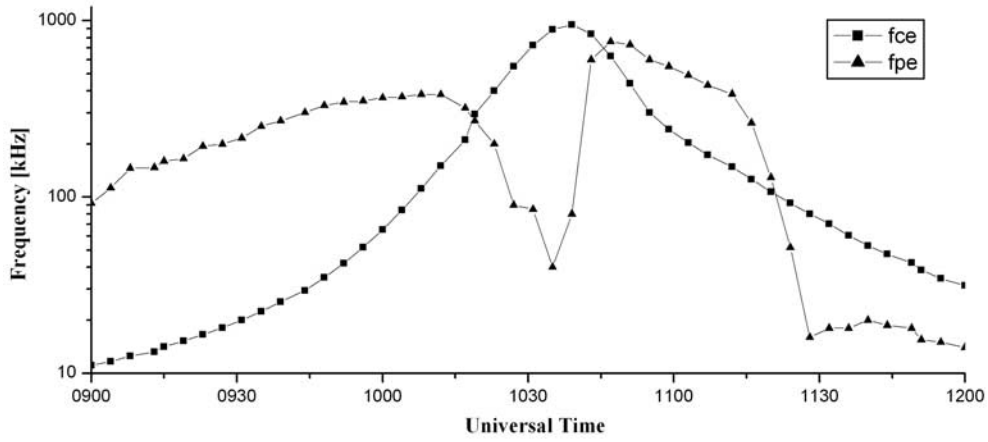

Figure 6. Plasma and electron gyro-frequencies measured by RPI on 29 September 2004.

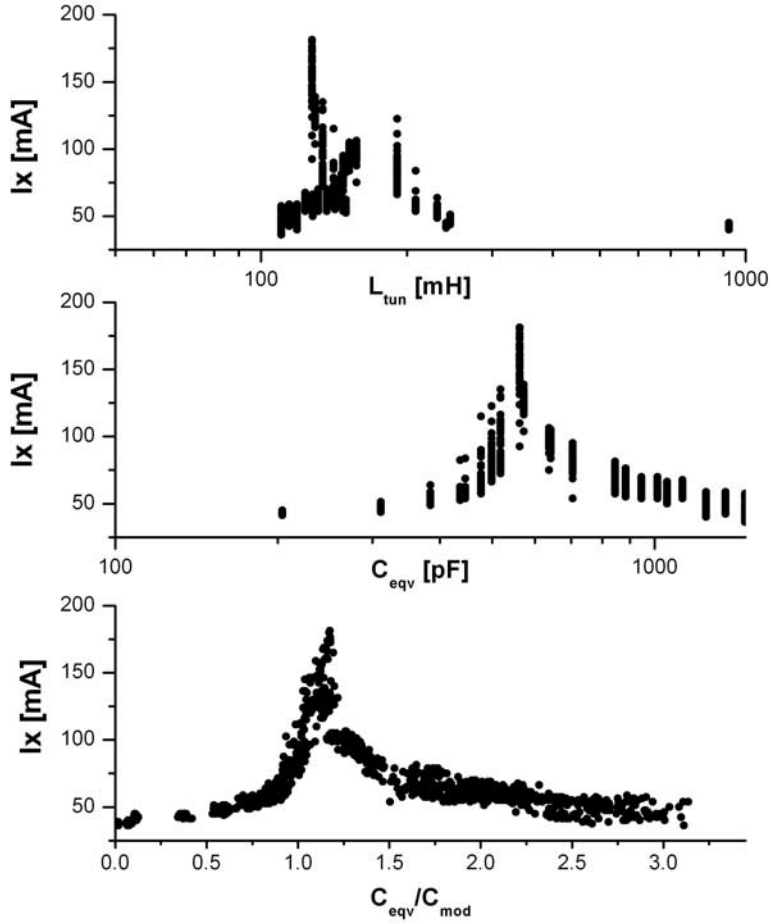

Figure 7. Current in the X-antenna as a function of the tuner inductance L_{tun} (top panel), equivalent capacitance $C_{eqv} = 1/\omega^2 L_{tun}$ (middle panel), and the normalized equivalent capacitance with respect to the model capacitance (lower panel).

However, the RPI transmitter supplies a maximum of 2 A at 50 V (Figure 1), i.e., 100 W of power. Therefore the current must be substantially out of phase with the voltage V_a on the antenna, leading to the conclusion that the antenna is highly reactive with a negligible current through the sheath conductance (sheath losses), or $1/\omega C_s \ll R_s + R_t + R_r$. It follows that the sheath reactance is around 3 kV/0.2A = 15 kΩ. At the frequency with maximum transmission, 19 kHz, the corresponding sheath capacitance is around 560 pF under the plasma condition when the maximum transmission occurred.

[34] One feature evident in Figure 5 is the positive correlation between the amplitudes of the antenna current and voltages as expected. The top panel of Figure 7 shows the current as a function of tuner inductance, L_{tun}, when each current value was measured. Each of the measurements satisfies the whistler mode condition; namely, the transmission frequency is less than both the local plasma and electron gyrofrequencies. Measurements with currents less than 0.05 A are not shown. Because there are only a limited number of inductances, there can be more than one measurement at each point on this plot. Similarly, since the transmission frequencies spread over a factor of 3, Figure 5, the currents at a single inductance correspond to several frequencies, different by up to a factor 3. The antenna was "in tune" when maximum current amplitudes were measured. The in-tune condition occurs when $L_{tun}C = 1/\omega^2$, where C and ω are the (total) sheath capacitance and the transmission angular frequency, respectively. The upper panel shows a complicated dependence of the current as a function of inductance because several frequencies shared the same inductance and only some of them were tuned to the system. An equivalent capacitance C_{eqv} is defined according to the in-tune condition. It represents the sheath capacitance only at current peaks. When the current is weak, it has no real physical meaning. The middle panel of Figure 7 shows the current as a function of equivalent capacitance. Because $C_{eqv} = 1/L_{tun}\omega^2$, different frequencies that shared the same inductance are now separated. A clear concentration of the in-tune condition appears in a range of the equivalent capacitances.

[35] The lower panel of Figure 7 shows the equivalent capacitance normalized by the capacitance based on our model, equation (29). If the model were perfect, there would be a single sharp peak at 1.0 of normalized capacitance in the lower panel. The first feature observation to note is that the normalization narrows the peak. The width of the peak, say the width at 100 mA, divided by the center value is

about 100% in the inductance panel and 40% in the equivalent capacitance panels, but it narrows to 30% for the normalized capacitance. The narrowing of the width of the peak from the top panel to the middle panel indicates that the effects due to different frequencies are removed to a certain degree. The further narrowing in the bottom panel indicates that the model capacitance correctly describes the capacitance as a function of plasma density. Note that the relatively smaller improvement from the middle panel to the lower panel is a result of the logarithmic dependence of the sheath capacitance on the plasma density, as shown in (15) and (25). The peak of the normalized capacitance is at about 1.2, indicating the model may underestimate the capacitance or overestimate the reactance by about 20%.

[36] The above comparison is based on the assumptions that the antenna was charged to a negative voltage close to the amplitude of the AC voltage (−3 kV) and that there is no electron sheath. Under these conditions, the cold electrons cannot penetrate the sheath and reach the antenna: hence the current in the sheath is negligible, there is no significant sheath conductance in the equivalent circuit (Figure 1). If the antenna were not fully charged, electrons would be accelerated when they move toward the branch with positive voltage and form the sheath current. This high-speed particle stream would bombard the antenna surface and produce heat on the antenna surface as the kinetic energy becomes thermal energy. According to the bare but uncharged antenna surface model, the equivalent resistance, referred to as sheath resistance in parallel with the sheath capacitance, is of the same order as the sheath reactance. In the experiment, the in-tune antenna current is about 0.2 A and the source voltage is 100 V at the secondary of the transmitter output transformer (Figure 1). The total equivalent circuit resistance, including the tuner resistance, leakage current effects, and radiation resistance, is 500 Ω. The inductor resistance is known to be 250 Ω. If the radiation resistance is of the order of 200 Ω based on the formula of *Balmain* [1964], the radiated power was I^2R_r = 8 W. When the antenna and the satellite are charged to −3 kV, the corresponding DC current associated with the ion motion attracted to the antenna and satellite is less than 2 mA (in parallel with the sheath capacitor and resistor, not shown in Figure 1), negligibly small compared with the transmission current. The approximation of neglecting the ion motion is therefore valid.

5. Summary and Discussion

[37] We have developed a first-principles-based model of the plasma sheath surrounding a bare antenna during whistler mode wave transmission. In this model, the antenna is negatively changed with a voltage similar to the amplitude of the driving voltage. An ion sheath is formed on each side of the antenna. The sheath is electron-free with little conduction current flowing through it. During a wave cycle, the radius of the sheath oscillates, translating to a current. This current is the current that radiates the wave into plasma. This picture is consistent with the displacement current of a capacitor. In addition to the DC electric charge to the bare antenna, the antenna charge also varies in time as the current decreases from the center to the tips. Differing from a conventional capacitor, for which the distance between the two plates is fixed, there is only one physical plate, which in our case is the antenna surface. On the other side, one may imagine a leaky surface of the sheath-plasma boundary which may play a similar role as a capacitor. However, the location of this surface oscillates in response to the charge variation on the antenna. Positive charges occur in the sheath. The net charge on the antenna and in the sheath is zero. On the plasma side, conduction current forms and radiates the wave.

[38] Equations are solved time-dependently in one-dimension by neglecting the magnetic field. The mathematical treatment includes the antenna DC charge and the radiation resistance. At the sheath-plasma boundary the voltage and the electric field cannot be zero at the same time or there would be no radiation. The analysis shows that at the sheath boundary, the electric field is zero. The electrons at the boundary will continue to move. As they are moving, the electric field is modified and so are the motions. Accordingly, the boundary moves at a varying speed. This motion of the boundary or the electron speed at the boundary gives the current for radiation.

[39] A whistler wave transmission experiment with the RPI instrument on IMAGE has shown that the model may describe the most important physical processes occurring in the system. It shows no evidence for any significant sheath (conduction) current or sheath conductance because the system appears to be highly reactive. The antenna is most likely charged to a substantial negative potential. Quantitatively, the model may underestimate the sheath capacitance by about 20%, leaving room for improvements.

[40] **Acknowledgments.** We thank G. Cheney of UML for implementing the RPI experiment and L. Chen of UC Irvine for helpful discussion. This work was supported by AFRL under contracts F19628-02-C-0092 and FA8718-05-C-0070 and by NASA under subcontract 83822 from SWRI.

[41] Amitava Bhattacharjee thanks Paul Kellogg and Daniel Sheehan for their assistance in evaluating this paper.

References

Abel, B., and R. M. Thorne (1998a), Electron scattering loss in the Earth's inner magnetosphere: 1. Dominant physical processes, *J. Geophys. Res.*, *103*, 2385.

Abel, B., and R. M. Thorne (1998b), Electron scattering loss in the Earth's inner magnetosphere: 2. Sensitivity to model parameters, *J. Geophys. Res.*, *103*, 2397.

Albert, J. M., D. H. Brautigam, R. V. Hilmer, and G. Ginet (2001), Dynamic radiation belt modeling at air force research laboratory, in *Space Weather*, *Geophys. Monogr. Ser.*, vol. 125, edited by P. Song, H. J. Singer, and G. L. Siscoe, p. 281, AGU, Washington, D. C.

Arbel, E., and L. B. Felsen (1963), Theory of radiation from sources in anisotropic media part 1: General sources in stratified media, in *Symposium on Electromagnetic Theory and Antenna*, edited by E. C. Jordan, p. 421, Pergamon, New York.

Balmain, K. G. (1964), The impedance of a short dipole antenna in a magnetoplasma, *IEEE, Trans Antennas Propag.*, *12*, 605.

Benson, R. F., V. A. Osherovich, J. Fainberg, and B. W. Reinisch (2003), Classification of IMAGE/RPI-stimulated plasma resonances for the accurate determination of magnetospheric electron density and magnetic field values, *J. Geophys. Res.*, *108*(A5), 1207, doi:10.1029/2002JA009589.

Burch, J. L., et al. (2001), Views of Earth's magnetosphere with the IMAGE satellite, *Science*, *291*, 541.

Despain, A. M. (1966), Antenna impedance in the ionosphere, *Rep. 3, AFCRL-66-412*, Upper Air Res. Lab., Univ. of Utah, Salt Lake City, Utah.

Garrett, H. B. (1985), The charging of spacecraft surfaces, in *Handbook of Geophysics and the Space Environment*, edited by A. S. Jursa, p. 1–7, Air Force Geophys. Lab., location?.

Grard, R. J. L., and J. K. E. Tunaley (1968), The impedance of the electric dipole aerial on the FR-1 satellite, *Ann, Geophys*, *24*, 1.

Inan, U. S., T. F. Bell, J. Bortnik, and J. A. Albert (2003), Controlled precipitation of radiation belt electrons, *J. Geophys. Res.*, *108*(A5), 1186, doi:10.1029/2002JA009580.

James, H. G. (2003), Electromagnetic whistler-mode radiation from a dipole in the ionosphere, *Radio Sci.*, *38*(1), 1009, doi:10.1029/2002RS002609.

Johnston, T. W. (1969), The low-frequency nonlinear current voltage characteristic for long dipoles mounted on ionospheric satellites, in *A Study of the VLF/ELF Satellite*, *Res. Rep., 7-801-80*, RCA, Montreal.

Kennel, C. F., and H. E. Petschek (1966), Limit on stably trapped particle fluxes, *J. Geophys. Res.*, *71*, 1.

Kivelson, M. G., and C. T. Russell (1995), *Introduction to Space Physics*, 568 pp., Cambridge Univ. Press, New York.

Laframboise, J. G., and L. W. Parker (1973), Probe design for orbit-limited current collection, *Phys. Fluids*, *16*, 629–636.

Langmuir, I., and H. M. Mott-Smith (1924), Studies of electric discharges in gases at low pressure, *Gen. Elec. Rev.*, *27*, 449–455.

Lyons, L. R., R. M. Thorne, and C. F. Kennel (1972), Pitch-angle diffusion of radiation belt electrons within the plasmasphere, *J. Geophys. Res.*, *77*, 3455.

Miller, E. K. (1967), The admittance of an infinite cylindrical antenna in a lossy incompressible anisotropic plasma, *Can, J. Phys.*, *45*, 4019–4038.

Mlodnosky, R. F., and O. K. Garriott (1962), The v.l.f. admittance of a dipole in lower ionosphere, paper presented at International Conference on the Ionosphere (London), Inst. of Phys. and Phys. Soc., Dorking, UK.

Oliver, B. M., R. M. Clements, and P. R. Smy (1970), The rf floating double probe as a plasma diagnostic, *J. Appl. Phys.*, *41*, 2117.

Reinisch, B. W., et al. (2000), The radio plasma imager investigation on the IMAGE spacecraft, *Space Sci. Rev.*, *91*, 319.

Reinisch, B. W., et al. (2001), First results from the radio plasma imager in IMAGE, *Geophys. Res. Lett.*, *28*, 1167.

Shkarofsky, I. P. (1972), Nonlinear sheath admittance, currents, and charges associated with high peak voltage driven on a VLF/ELF dipole antenna moving in the ionosphere, *Radio Sci.*, *7*, 503.

Song, P., H. J. Singer, and G. L. Siscoe (Eds.) (2001), *Space Weather*, *Geophys. Monogr. Ser.*, vol. 125, AGU, Washington, D. C.

Wang, T. N., and T. F. Bell (1972), VLF/ELF radiation patterns of arbitrarily oriented electric and magnetic dipoles in a cold lossless multicomponent magnetoplasma, *J. Geophys. Res.*, *77*, 1174.

K. Bibl, I. Galkin, X. Huang, V. Paznukhov, B. W. Reinisch, G. Sales, P. Song, and J.-N. Tu, Center for Atmospheric Research, University of Massachusetts, Lowell, 600 Suffolk Street, Lowell, MA 01854-3629, USA.

D. Cooke, Air Force Research Laboratory, Space Vehicles Directorate, 29 Randolph Road, Hanscom Air Force Base, MA 01731-3010, USA.